Geochimica et Cosmochimica Acta, Vol. 69, No. 10, pp. 2517–2533, 2005

0016-7037/05 $30.00 + .00

doi:10.1016/j.gca.2004.12.001

Authigenic calcium carbonate flux in groundwater-controlled lakes: Implications for lacustrine paleoclimate records

M. D. Shapley,[1,*] E. Ito,[1] and J. J. Donovan[2]

[1]Limnological Research Center, Department of Geology and Geophysics, University of Minnesota, 310 Pillsbury Drive SE., Minneapolis, Minnesota 55455 USA
[2]Department of Geology and Geography, West Virginia University, 425 White Hall, Morgantown, West Virginia 26506 USA

(*Received December* 23, 2003; *accepted in revised form December* 9, 2004)

Abstract—Groundwater dominated lakes are an important feature of many landscapes. Their sediments are a particularly valuable source of paleoenvironmental information in semiarid regions where perennial lakes may otherwise be scarce. Where groundwater and lake composition are favorable, carbonate mineral precipitation, evaporative concentration of lake water, and microbial processes can combine to strongly deplete dissolved Ca relative to influent groundwaters. The authigenic carbonate flux (ACF) can then become limited by water column cation availability and thereby be coupled to groundwater inflow rates and aquifer recharge. Here we analyze sedimentary records from two marl-producing, groundwater-controlled lakes and demonstrate a link between one-dimensional ACF and the Palmer Drought Severity Index (PDSI), a measure of land surface wetness. In a restricted outflow lake with high-carbonate alkalinity, ACF is enhanced during historically wet climatic periods in response to increased aquifer recharge rates. ACF in this lake declines during droughts. A neighboring dilute lake with a high rate of groundwater outflow shows comparatively weak coupling between ACF and PDSI history. Ionic chemistry, carbonate mineral equilibria, and $\delta^{13}C$ patterns of dissolved inorganic carbon show that the sensitivity of the ACF signal depends on the degree of evaporative evolution of lake water and the mineral saturation state of the water column under conditions of stratification and ice cover.

1. INTRODUCTION

Many investigations of continental paleoclimate employ indirect information, or proxies, preserved in chemically or biogenically precipitated lacustrine carbonate sediments. Such proxies have the potential to quantitatively record paleolake water isotopic and solute composition, both of which are closely linked to the changing hydrologic status of the surrounding watershed (McKenzie and Hollander, 1993; Benson et al., 1996; Ito, 2001; Last, 2001). In semiarid landscapes, fluid and solute balances of perennial lakes frequently have a strong groundwater component. Such "groundwater effects" are often viewed as a source of unwanted complexity in lacustrine paleorecords. Where paleorecord interpretations explicitly consider groundwater dynamics, however, the results can clarify questions both of environmental change and hydrologic process (Teller and Last, 1990; Sanford and Wood, 1991; Rogers and Dreiss, 1995; Smith et al., 1997; Donovan et al., 2002). New evaluations of the manner in which groundwater processes are reflected in paleorecords are therefore of interest. Here we examine late Holocene paleorecords from two lakes in which authigenic carbonate production may be supported and limited by groundwater exchange. We attempt to quantitatively relate authigenic mineral flux to groundwater supply rate and, thereby, to climate.

* Author to whom correspondence should be addressed (shap0029@umn.edu).

2. HYPOTHESES AND PURPOSE

Groundwater-dominated lakes receive solutes primarily from groundwater inflow. Calcium ± magnesium may react with dissolved inorganic carbon (DIC) to precipitate as authigenic carbonate minerals such as calcite, aragonite, and dolomite (Dean, 1981; Last, 1982; Mucci and Morse, 1983; Donovan, 1992). At high lake alkalinity and pH, carbonate mineral phases may precipitate to the point of solute limitation of the cation and may strongly deplete lake Ca activities relative to inflowing groundwater (Eugster and Hardie, 1978; Eugster and Jones, 1979; Sanford and Wood, 1991; Donovan, 1992). Under such Ca-limited conditions, we hypothesize that mass rates of $CaCO_3$ formation should be quantitatively linked to locally prevailing rates of groundwater and Ca inflow, provided there are no other important sinks for Ca in the lake ecosystem or sediment.

Groundwater fluxes and lake-aquifer fluid exchanges are strongly controlled by climate, and in particular, groundwater recharge is sensitive to rates and seasonality of meteoric precipitation (Winter, 1983; Sophocleous and Perry, 1985; Winter, 1999). We therefore propose that the mass rate of limnic $CaCO_3$ formation, or authigenic carbonate flux (ACF), is linked to climate and is a plausible paleorecharge metric in geochemically appropriate lakes. If so, ACF should increase during climatically wet periods when aquifer recharge is enhanced as suggested by Teller and Last (1990). Anomalies in recent ACF should then be correlative with historical records of climate that reflect recharge availability. ACF enhanced by groundwater recharge in this way should contrast with that predicted where

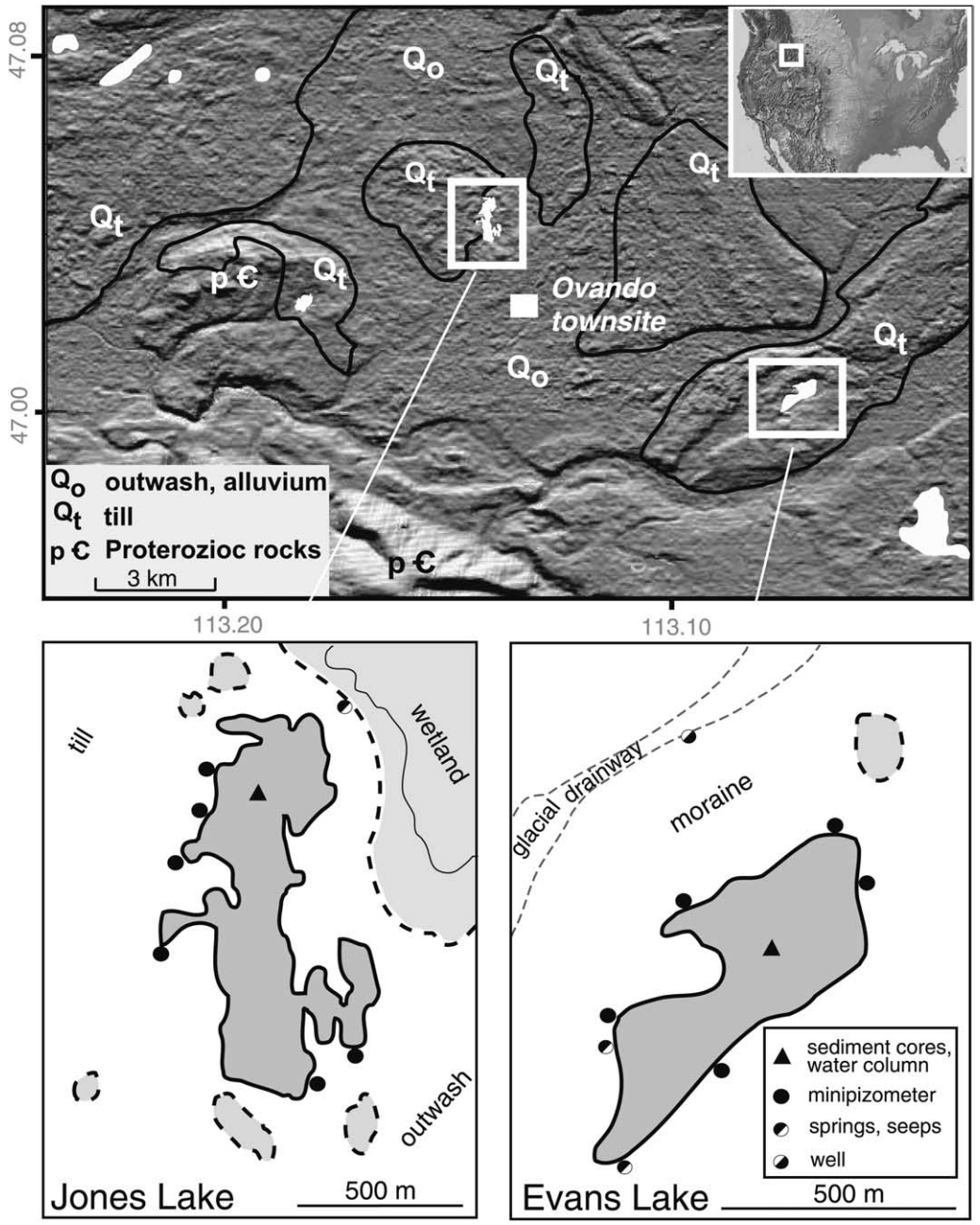

Fig. 1. Lake setting and sampling locations, Ovando, Montana, United States.

carbonate mineral production is controlled primarily by lake evaporation or phytoproductivity.

Several factors may complicate the interpretation of lake sediment records in terms of groundwater fluxes and ACF. Detrital sediment can provide an additional carbonate mineral flux which, if significant, could mask the ACF signal. Sediment focusing and other depositional factors make integration of sediment masses over a lake basin difficult. Heterogeneity in groundwater composition makes source-water chemistry difficult to characterize. Notwithstanding these complications, we propose that ACF may provide a valuable paleohydrologic tool when applied in appropriate settings.

Here, we test this hypothesis against 20th century sediment geochemistry and climatic records from a lake district in the Northern Rocky Mountains of Montana, United States. Using carefully dated sediment sequences from two geochemically contrasting lakes responding to similar climate forcing, we demonstrate the potential utility, data requirements, and limitations of ACF as a paleohydrologic tool.

3. RESEARCH SETTING AND METHODS

3.1. Regional Geologic Setting

The Ovando Valley is a structural basin of the Northern Rocky Mountains underlain by a complex of Late Wisconsinan glacial and

Table 1. Summary limnological characteristics of field sites.

	Evans Lake	Jones Lake
Surface elevation, 8/2000	1279.9 m (MSL)	1248.3 m (MSL)
Surface area, 8/2000	2.57 E5 m^2	3.22 E5 m^2
Maximum depth, 8/2000	7.7 m	12.5 m
Mean depth, 8/2000	2.37 m	2.46 m
Volume, 8/2000	6.08 E5 m^3	7.84 E5 m^3
Dissolved solids range	186–277 mmol/l	2.48–6.68 mmol/l
Mg:Ca range	100–500	.5–1.5
pH range	8.8–9.5	6.6–9.0
Hydraulic residence time	8–9 years	1.5–2 years
Dominant outflow	evaporation	groundwater

MSL: mean sea level

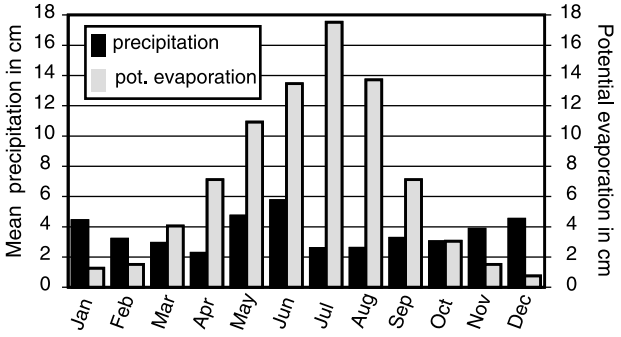

Fig. 2. Seasonal precipitation history for the Ovando climate station (National Climate Data Center station number 246302; period of record 1900 to 1975) and calculated monthly potential evaporation based on climatic data for the period 1940 to 1970 (MAPS, 2003).

glaciofluvial sediments. Three coalescing piedmont ice lobes occupied portions of the valley during the late Glacial. Final wasting of these ice masses left a landscape of poorly integrated basins, steep moraines, and knobs distributed across the valley floor (Dea, 1981; Fig. 1). Relatively thin (<50 m) Quaternary sediments are underlain by thick clastic sequences of mid-Tertiary age (Tuck et al., 1996). Metasedimentary rocks of the Proterozoic Belt Supergroup are exposed in the surrounding uplands and floor the basin.

3.2. Regional Hydrologic Setting

Quantitative analyses of groundwater flow within the Ovando Valley are lacking, but inferences can be drawn from regional evaluations (e.g., Tuck et al., 1996) and from our field observations. Water supply wells encounter aquifers within Holocene alluvium, Quaternary-aged glacial deposits, and in the upper 100 m of Tertiary-aged sediments. Regionally, groundwater potentials are high around the valley margins and decline toward the valley center; areas of flowing wells along major streams (the Blackfoot River and the North Fork Blackfoot River) indicate upward potentiometric gradients and likely regional groundwater discharge in low-elevation areas. Locally, lakes occur within areas of poorly integrated drainage and steep slopes. We infer this topography superimposes complex local flow systems on the regional groundwater flow pattern.

Based on evaluations of limnologic and geochemical data, we selected two perennial lakes (Jones Lake and Evans Lake) for evaluation of the link between ACF and climatically controlled groundwater recharge. The two lakes are similar in surface area, volume, and topographic catchment and are exposed to similar evaporative forcing (Table 1). The lakes lack both surface water outflow and organized surface water inflow; neither displays geomorphic evidence of past wet-period spills.

At Jones Lake, elevated and topographically complex terrain to the west of the lake probably provides locally focused groundwater recharge contributing to observed lakeshore discharge. To the south, a well-drained outwash surface encourages enhanced recharge from water management activities discussed later. To the east and northeast, stream incision has formed an abrupt 10 m slope below the lake. Copious year-round spring flow along the base of this slope carries the isotopic signature of Jones Lake and clearly indicates lake outflow. At Evans Lake, elevated terrain to the north, west, and south likely provides recharge to local flow systems intersecting the lake; lakeshore groundwater discharge can be observed in each of these lake quadrants.

Euro-American settlement in the latter 19th century brought changes in land use. Livestock grazing was established in the area by AD 1890 with probable but undocumented changes in vegetation cover and aquatic nutrient cycling. Between AD 1910 and 1920, parts of the Jones Lake watershed were cultivated (wheat), the Evans Lake watershed remained in forest and pasture. By the 1930s, land use surrounding Jones Lake reverted to livestock grazing. However, an irrigation ditch originally constructed early in the 20th century and supplied by a small stream to the east of Jones Lake remains in place. During the 1980s and 1990s, the landowner used this ditch to import water to a small kettle formed in outwash gravels 150 m south of Jones Lake, seasonally raising water levels by as much as 5 m. Enhanced groundwater influx driven by this artificial aquifer recharge has resulted in Jones Lake water levels exceeding those experienced previously.

3.3. Regional Climatic Setting

Archival climatic data for the community of Ovando, centrally located within the region of lakes, show the Ovando Valley experiences two seasonal precipitation maxima of similar amplitude (Fig. 2). A winter maximum reflects Pacific moisture transport and results in a seasonal snowpack that melts from the valley floor in March and April. Early summer precipitation is delivered through May and June thunderstorm activity coincident with the precipitation maxima of the northern Great Plains (Bryson and Hare, 1974; Mock and Bartlein, 1994). Mean annual precipitation for the period 1900 to 1975 was 43 cm, with 44% occurring during the typical months of snow accumulation (November–March). Time-averaged evaporation exceeds precipitation, consequently most small basins lack surface water outflow. Regionalized Penman estimates of annual potential evaporation are near 82 cm for the Ovando Valley (MAPS, 2003). Of the calculated potential evaporation, 11% is attributed to the November to March period when ice cover normally precludes actual lake evaporation. Class A evaporation pan data collected 8 km northwest of Jones Lake during 1998 and 1999 show growing season totals of 99 and 84 cm (Cook, 2001), generally consistent with regionalized potential evaporation values.

3.4. Sampling and Analytical Methods

3.4.1. Sediment

In 1997, we collected ~1-m long sediment cores from profundal sites in both lakes using a manual polycarbonate piston corer. Cores were extruded in 2 cm increments on-site and stored in watertight sample cups. Subsampling for water content and ^{210}Pb analysis occurred within 20 days of sample collection. Lead-210 was measured through its granddaughter product ^{210}Po, with added ^{209}Po used as an internal yield tracer. Unsupported ^{210}Pb activity was calculated by subtracting supported activity from total activity, with supported activity estimated from the asymptotic activity at depth in the core. Lead-210 measurements were reduced according to a constant rate of supply (CRS) model (Appleby and Oldfield, 1978) to generate depth-age and sediment mass flux curves for the two sites. Confidence intervals on ^{210}Pb ages were calculated by first-order error analysis of counting uncertainty (Binford, 1990).

The CRS model assumes that the flux of unsupported ^{210}Pb to the sediment surface is constant, while the initial concentration of ^{210}Pb varies with changes in total sedimentation rate. The CRS model provides a reliable basis for interpreting ^{210}Pb profiles in lakes where the watershed contribution of ^{210}Pb is small and depositional hiatuses are absent (Appleby, 2001). Here, the lack of stream inflow and small drainage basin to lake-area ratios indicate watershed ^{210}Pb is unlikely

to result in important errors. Sedimentology and local oral history indicate these lakes have been perennial during the period considered by our analysis.

Sediment subsamples for carbon and mineralogical analyses were split from the homogenized field samples and freeze-dried. Total inorganic carbon (TIC) and total carbon (TC) analyses were performed on a UIC, Inc. coulometric carbon analyzer. Total organic carbon (TOC) was calculated as the difference between TC and TIC. We performed replicate analyses on 15% of field samples; replication is generally within 2% of sample concentration. ACF was calculated as the product of TIC, the gross sediment flux determined from ^{210}Pb, and the mass ratio of $CaCO_3$ to C.

Determinations of mineral concentrations were made by X-ray diffraction (XRD). Analyses were performed on a Phillips Model 1200 Diffractometer using Cu Kα radiation. Freeze-dried samples were ground in an agate mortar and mounted with random orientation into 2.4 cm epoxy disks. Mineral identification was done using automated peak search, and peak areas were quantified against standards for quartz, calcite, aragonite, dolomite, and chlorite. The XRD results for aragonite, calcite, and dolomite were indexed to the coulometric carbonate mineral fraction to improve precision. Smear slides of whole sediment from selected core intervals were prepared and examined for petrographic determination of sediment composition and textures.

3.4.2. Aqueous chemistry

Ovando-area waters were systematically sampled for geochemical composition from 1997 through 2002. In particular, sampling included seasonal water column profiling of Jones and Evans lakes and sampling of groundwater from wells and shallow minipiezometer placements (Winter et al., 1988) in littoral areas. Field analyses included measurements of pH, temperature, dissolved oxygen, and alkalinity. Laboratory analyses included major ions, selected trace elements, and ^{13}C of dissolved inorganic carbon ($^{13}C_{DIC}$). Analyses of $^{87}Sr/^{86}Sr$ were performed on a selected subset of lake and groundwater samples. These data are the basis for solute and isotope balance analyses of lake source composition and lake/groundwater fluxes, as well as equilibrium modeling of mineral authigenesis.

Water column measurements were collected in situ using a Hydrolab multisensor probe calibrated daily for pH, specific conductance, and dissolved oxygen. Lake water samples were collected using either a Van Dorn sampling bottle or a peristaltic sampling pump, and acid-washed Tygon tubing. Groundwater samples were obtained from minipiezometer installations by peristaltic pumping, following purging to "develop" the screened minipiezometer point. Following discharge of one or more casing volumes of water, production wells were sampled at the wellhead or at the most upstream available discharge point. Spring waters were directly sampled from the most upgradient point of discharge.

Samples for ionic analyses were passed through 0.45 μm membrane filters. Samples for cation analyses were stabilized with high-purity HNO_3^- or HCl (pH <2) in acid-washed Nalgene bottles. Samples for analysis of $^{13}C_{DIC}$ were immediately crimp-sealed in dark glass bottles with Teflon septa. All water samples were ice-packed or refrigerated until analysis.

Cation analyses were performed by inductively coupled plasma mass spectroscopy (ICP-MS; Elmer/Sciex Elan 5000 and Thermo Elemental VG instruments) with precision of 2% or better. Anions were analyzed by ion chromatography on a Dionex instrument calibrated daily to five standard solutions per ion.

Analyses of $^{13}C_{DIC}$ (as CO_2 gas) were conducted on one of two instruments: a Finnigan-MAT Delta E multicollector, dual inlet mass spectrometer, or a Finnigan-MAT 252, both with analytical precision of 0.2‰. CO_2 gas generation from sample waters was by direct acidification with 105% anhydrous H_3PO_4 (Graber and Aharon, 1991). Compositions are expressed relative to the Vienna Pee Dee Belemnite (VPDB) standard.

Filtered, unacidified samples were centrifuged and purified with conventional ion-exchange methods and loaded on single Ta filaments with H_3PO_4 for measurement of $^{87}Sr/^{86}Sr$ composition. Isotope ratios were measured with an automated VG54 sector multicollector thermal ionization mass spectrometer in dynamic mode. Mass dependent fractionation was corrected assuming a $^{86}Sr/^{87}Sr$ of 0.1194. Strontium isotope ratios are reported relative to SRM-987 standard value of 0.71025.

We evaluated carbonate mineral saturation states and mixing behavior of water using the extended Debye-Huckel equations as implemented by the Geochemist's Workbench software package (Bethke, 2002). Ionic strength of Evans Lake water ($\sim$.2 mol) approaches but does not presently exceed the limits of usefulness for the extended Debye-Huckel model (Langmuir, 1997). Input parameters include field measurements of pH and temperature and laboratory measurements of ion concentrations. Inorganic carbon species were determined from field alkalinity titrations and from calibrated gas pressures generated during inorganic carbon extractions for $\delta^{13}C_{DIC}$, distributed according to field measurements of pH and equilibrium constants for dissolved CO_2. Samples with charge-balance errors exceeding an absolute value of 10% are excluded from mass balance analyses. Dissolved CO_2 is calculated from the activity of H_2CO_3 and the temperature-dependent equilibrium constant for the dissolution of CO_2 in water (Langmuir, 1997). Mixing calculations first equilibrate averaged groundwater compositions to lake pCO_2 conditions, then progressively titrate groundwater into lake water in the presence of $CaCO_3$ while tracking changes in solute inventory and mineral production.

Steady state lake mass balance estimates are keyed to Cl^- concentrations of lakes and inflowing groundwaters after the method of Donovan (1994). Chloride is assumed to behave conservatively. Solute fluxes are calculated as groundwater influx, groundwater outflow, and a "reaction flux" or source/sink term (Table 2). Here the reaction flux represents the sum of multiple processes including the sequestering of authigenic minerals in lake sediment and loss of gas phases to the atmosphere.

3.4.3. Climatic history

We used the regionalized Palmer Drought Severity Index (PDSI) reconstruction of Cook et al. (1999) for a hydroclimatic metric. The PDSI uses a rule-based water balance model of surface water exchange to define a dimensionless wetness index reflecting the duration and intensity of departures from regional mean conditions (Alley, 1984). While the PDSI has various limitations (Alley, 1984; Alley, 1985; Keyantash and Dracup, 2002), the index integrates parameters that reflect availability of water moving through the vadose zone to the water table. This reconstruction of 20th century PDSI integrates climatic data from several nearby stations centered on the Ovando Valley, mitigating problems of data completeness in the Ovando climate station record.

3.4.4. Data reduction

Time series of ACF and PDSI are both represented as departures from a mean state, detrended by application of a linear fit to the raw data. Jones Lake underwent an abrupt offset in carbonate flux related to water management changes affecting recharge rates. Therefore, these data were detrended in two segments, before and after the early 20th century disturbance. Mean values and standard deviations for the detrended data sets were used to normalize scalar values, yielding time series of serial, noncumulative departures from mean values, expressed in terms of standard deviations (Z scores).

4. RESULTS

4.1. Limnology and Lake Water Column Structure

Evans and Jones lakes display strong seasonality in thermal and chemical structure, summarized for the yr 1999 to 2001 in the electronic annex (EA1). By early summer, both lakes display strong water column stratification. Near-complete consumption of dissolved oxygen by microbial respiration below the thermocline produces reducing hypolimnetic conditions. Epilimnetic waters of both lakes remain oxic. Hypolimnetic CO_2 production through organic matter mineralization results in pH depression; pH in Jones Lake may drop to $\sim$6.6 under stratified conditions, while Evans Lake water column pH gen-

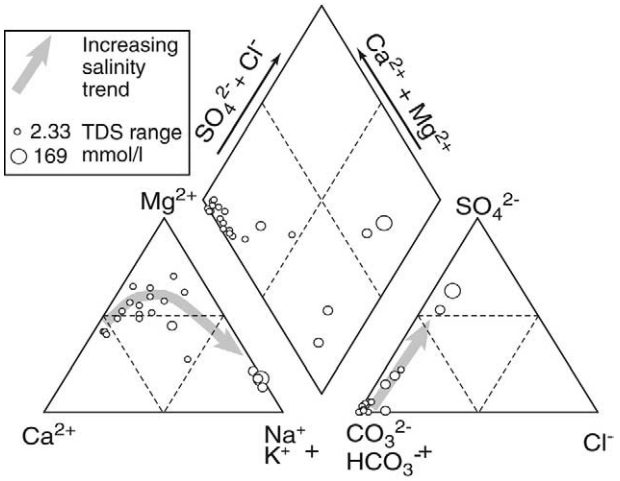

Fig. 3. Ionic compositions of lake and wetland water in the Ovando area ($n = 22$). Symbol size is proportional to the log of total dissolved solids.

erally falls no lower than 8.5 near the sediment interface. The Evans Lake hypolimnion becomes pungent with H_2S under stratified conditions; H_2S odors are not detected in Jones Lake. Downward propagation of the mixed zone of both lakes may leave only thin, low-volume hypolimnia by late summer (for example, Jones Lake, September 2000; Evans Lake, September 1999). Autumn overturn, probably occurring in October of most yr, homogenizes lake pH and oxygenates the full water column.

Ice cover generally develops on both lakes in November and persists into April. In Evans Lake, ice cover appears to promote near-depletion of dissolved oxygen by early in the winter (for example, January 2000); water column pH remains high (8.5 and above). In Jones Lake, dissolved oxygen in the mg/L range persists in the upper water column through the season of ice cover. CO_2 production from oxidation of organic matter at or near the sediment interface lowers water column pH to near 7 before loss of ice cover.

4.2. Aqueous Chemistry

Evaporation acting on water bodies subject to contrasting hydrogeologic controls produces a wide diversity of lake and wetland salinity in the Ovando area. Lake concentrations range from <2.5 mmol to ~1000 mmol total dissolved solids (TDS). Due to carbonate mineral precipitation, concentrated water bodies evolve along an alkaline, Ca-depleted pathway leading from dilute Ca-HCO3 groundwater to brackish Na-SO_4 lake compositions (Fig. 3). Evans and Jones lakes show contrasting degrees of evolution from similar groundwater inflow compositions (Fig. 4). TDS of Evans Lake exceeds that of Jones Lake by a factor of 40 to 50. Accompanying the contrasting salinity of the two lakes is a systematic contrast in ionic composition consistent with trends seen in numerous lakes and ponds across the Ovando Valley. Higher salinities correlate with high values of SO_4:(HCO_3^- + CO_3^{2-}) and Mg:Ca and high ratios of Na and K to Ca and Mg.

This trend is explained by compositional movement along the chemical pathway IIIA of Hardie and Eugster (1970), accompanying $CaCO_3$ precipitation from initial solutions where molar HCO_3^- moderately exceeds Ca^{2+}. Initial precipitation of $CaCO_3$ occurs in response to CO_2 loss from inflowing supersaturated groundwater and photosynthetic uptake of CO_2. As evaporative concentration proceeds, increasing HCO_3^- concentrations drive Ca^{2+} downward, shifting cation dominance toward Mg^{2+}, Na^+, and K^+. Ca removal by carbonate mineral formation prevents these waters from reaching saturation with gypsum, so SO_4^{2-}, present at low concentrations in source waters, becomes the dominant anion at high lake concentrations (Fig. 4; EA2). Where SO_4^{2-} concentrations are high, evidence of microbial sulfate reduction (H_2S production in sediments and hypolimnia) becomes prominent. Widely varying lake residence time produces the broad distribution of lake salinity and ionic dominance shown.

Results of $^{87}Sr/^{86}Sr$ and Sr analyses show distinct compositions for groundwater from Quaternary sediments ($^{87}Sr/^{86}Sr > 0.72$) and from Tertiary wells ($^{87}Sr/^{86}Sr < 0.71$). Evans Lake $^{87}Sr/^{86}Sr$ (0.7189) is intermediate between Quaternary and Tertiary groundwater compositions, indicating mixing of low-$^{87}Sr/^{86}Sr$ Tertiary water with the more apparent Quaternary groundwater inflow to the lake. We believe the Cone well (EA2) represents the most probable low-$^{87}Sr/^{86}Sr$ end member

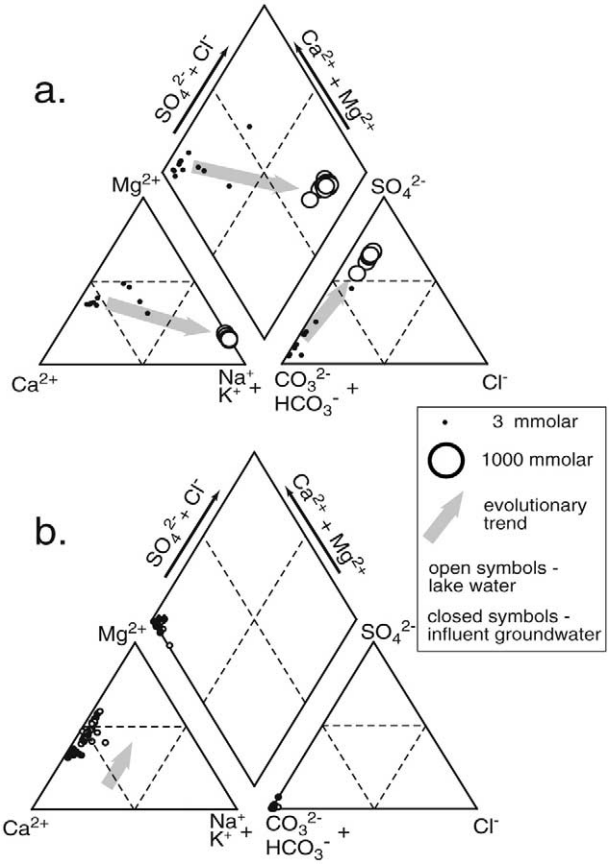

Fig. 4. Major ion compositional shifts in lake waters from initial groundwater chemistries: (a) Evans Lake evolution resulting from aragonite precipitation, evaporative concentration, and sulfate reduction; (b) Jones Lake evolution resulting from seasonal calcite precipitation and minimal evaporative concentration.

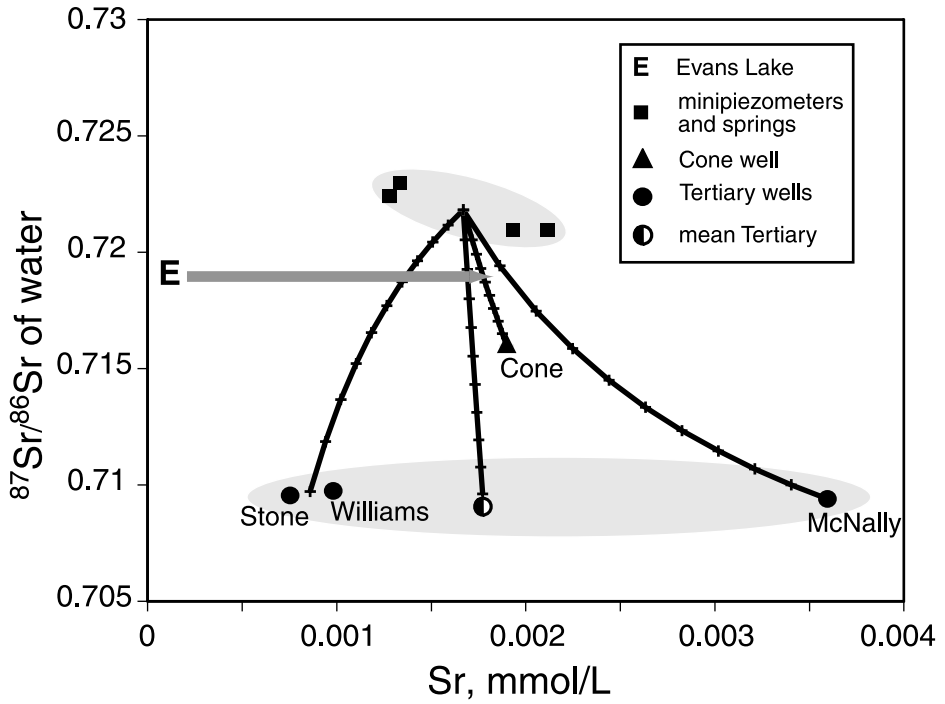

Fig. 5. $^{87}Sr/^{86}Sr$ composition of lakes and groundwater and calculated mixing curves between shallow (minipiezometer) and possible deeper groundwater end-member compositions. Mixing curves are calculated according to Faure (1986). Evans Lake Sr concentration is low relative to all groundwater compositions due to probable uptake by precipitated aragonite. Evans Lake $^{87}Sr/^{86}Sr$ composition extrapolates along the Sr concentration axis to points of intersection along the mixing curves; tic marks represent increments of 10% Tertiary groundwater contribution, increasing downward. Lake mass balance estimates use the minipiezometer (52%)/Cone well (48%) intercept as the weighted groundwater inflow composition.

for mixed inflow to Evans Lake. Two-component mixing curves calculated according to Faure (1986) suggest 48% of Evans Lake groundwater inflow may be represented by the Cone well composition. Figure 5 summarizes our interpretation of lake inflow mixing based on the $^{87}Sr/^{86}Sr$ and Sr data.

4.3. Sedimentology and Authigenic Carbonate Flux

4.3.1. Evans Lake

Lead-210 activity in the Evans Lake core decreases monotonically down-core to reach a supported activity of 0.3205 pCi/g at a depth of 44 cm below the sediment/water interface. One-sigma errors are ± 3 to 6 yr in the late 19th and early 20th centuries. The constant rate of supply (CRS) model fitted to these data yields dry-mass sedimentation rates from ~0.01 to 0.03 g/cm^2/yr. The resulting age-depth model is presented in Figure 6; activity data, age, and calculated sedimentation rates are found in Table 3.

Sediments of the Evans Lake core consist of fine-grained, laminated, aragonitic mud and aragonite ooze (sensu Schnurrenberger et al., 2003). Authigenic aragonite occurs as fine (2–5 μm) subhedral, elongated prisms, needles, and rice-shaped grains. Subordinate calcite occurs as short prisms and spheroids, rarely as "dumbbells" and radial agglomerations.

There are two readily recognized lithostratigraphic units within the Evans Lake core (Fig. 6). The upper 32 cm (unit 1) is laminated, dark brown aragonite mud with total organic carbon (TOC) of 12 to 25% and quartz (detrital) between 15 and 40% of mineral mass. Underlying this unit is 70 cm of laminated aragonite mud and aragonitic algal ooze speckled with Fe-sulfide agglomerations 0.5 to 5 mm in dimension (unit 2); TOC ranges from 15 to >30%, and quartz is typically <15% of mineral mass. Freshly exposed core surfaces are black and smell strongly of H_2S.

Figure 7 shows variations in carbon (TOC and TIC) and mineralogy of the Evans Lake core. Lithostratigraphic units 1 and 2 show contrasts in sediment composition that correlate with the advent of agricultural activities. The upward transition to unit 1 (32 cm; ca. AD 1895) is marked by a decrease in % TOC and % TIC, a moderate increase in detrital mineralogy (quartz + feldspars), and commensurate dilution of authigenic aragonite.

4.3.2. Jones Lake

Lead-210 activity in the Jones Lake core decreases systematically down-core to reach a supported activity of 0.3256 pCi/g at a depth of 69 cm. Calculated dry-mass sedimentation rates range from ~0.023 to 0.074 g/cm^2/yr (Table 3).

Sediments of the Jones Lake core comprise a sequence of fine-grained, banded calcite mud, calcareous silt, and diatom ooze. Authigenic calcite occurs primarily as euhedral prisms, rhombs, and spheroids up to 25 μm in dimension and secondarily as equant, subhedral, and anhedral grains less than 5 μm in dimension. As with Evans Lake, we recognize two lithostratigraphic units (Fig. 8). The upper 45 cm (unit 1) is a dark

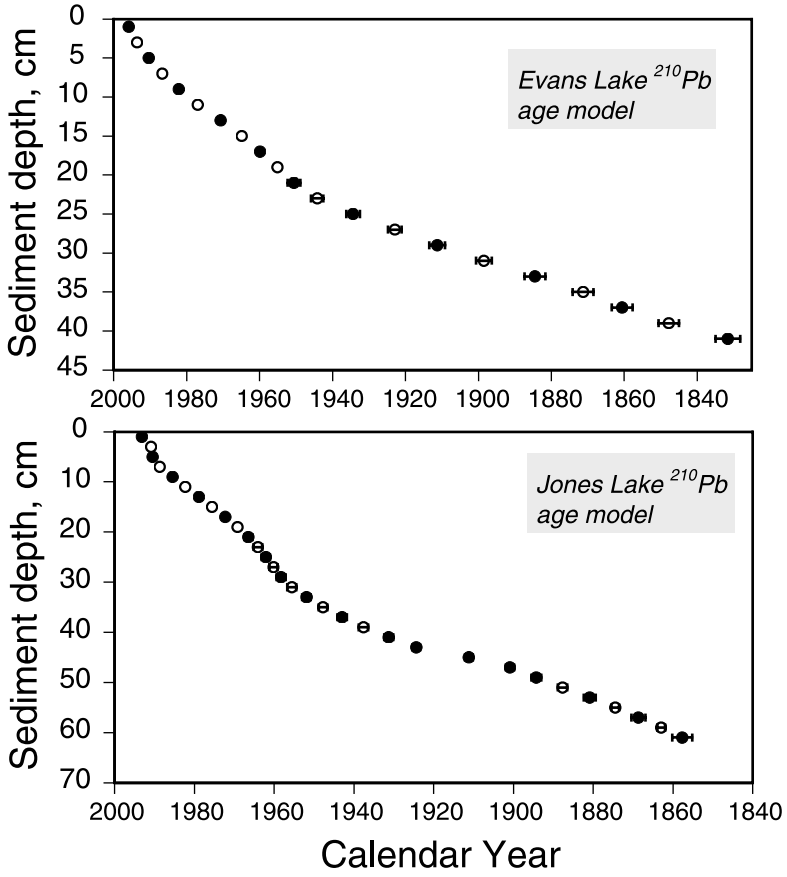

Fig. 6. Lead-210 depth-age models for the Evans Lake and Jones Lake cores. Open symbols are points interpolated according to the constant rate of supply (CRS) model. Supported ^{210}Pb is calculated as 0.32 pCi/g in both cores. One-σ age errors were calculated by first-order error analysis of counting uncertainty (Binford, 1990). (Where error bars are invisible, age error is exceeded by symbol size.)

brown, faintly laminated calcareous diatom ooze with TIC of ~0.6 to 2%. Underlying unit 1 are >45 cm of dark brown to grayish brown calcite mud and calcareous silt, banded at a scale of 50 to 20 mm and with 3 to 5% TIC (unit 2). Unit 2 is punctuated with occasional centimeter-scale diatom oozes dominated by *Asterionella* frustules.

Compared to Evans Lake, Jones Lake sediments show similar but stronger contrasts between lithostratigraphic units. The upward transition from unit 2 to unit 1 entails an increase in % TOC and a transient increase in detrital mineralogy. More intensive agricultural land use resulted in a more pronounced sedimentological imprint of Euro-American settlement than at Evans Lake.

4.3.3. Authigenic fluxes and climate

Figure 9 shows the relationship between departures of ACF and PDSI for the 20th century in Evans and Jones lakes. Within the error of the Evans Lake ^{210}Pb chronology, all ACF departures with magnitude exceeding 0.5 standard deviations of the mean correspond temporally to PDSI departures. Consistent with the concept of cation-supply limitation of ACF, enhanced land surface moisture corresponds to positive anomalies in the flux of authigenic aragonite. Drought corresponds to decreased authigenic flux. Figure 9a shows only a moderately strong correlation between the magnitude of climatic and sediment-flux anomalies ($r^2 = 0.49$), likely reflecting the influence on recharge rates of variables not incorporated into the PDSI.

The Jones Lake record indicates a weaker relationship between calcite sediment flux and PDSI anomalies (Fig. 9b). Broad features of the PDSI curve before 1980 are reflected in the ACF departure record. Sensitivity is low, however, and over the last 20 yr of the record, PDSI and carbonate flux anomalies appear to correlate negatively, contrary to the groundwater flux model.

4.4. Dissolved CO_2 and $\delta^{13}C$ of Inorganic Carbon

Apparent partial pressures of CO_2 calculated for Ovando lakes and groundwaters are summarized in Figure 10. Apparent pCO_2 is normalized with respect to atmospheric CO_2 pressure and plotted against $\delta^{13}C$ of DIC. Jones Lake and Evans Lake minipiezometer samples show largely overlapping fields. Apparent pCO_2 is one to two orders of magnitude above atmospheric; low $\delta^{13}C_{DIC}$ reflects vegetative sources of groundwater DIC (Fritz et al., 1978; Wachinew and Rozanski, 1997). Naturally discharging shallow groundwater from a perennial spring also falls within the field defined by minipiezometer data. Wells drawing water from deeper

Table 2. Estimated solute mass balances for exchange of groundwater with Evans Lake (upper) and Jones Lake (lower).

	C(i) Groundwater composition 48% Cone mg/l	C(1) Evans Lake all samples 1997–2001 mg/l	C(1)/C(i) α	α(i)/α(Cl) π	C(0) mol/m**3	C(1) mol/m**3	Inflow flux mol/yr q	Outflow flux mol/yr s	Reaction flux mol/yr r
Ca	6.53E + 01	4.10E + 00	6.28E − 02	2.99E − 04	1.63E + 00	1.03E − 01	1.26E + 05	3.77E + 01	1.26E + 05
Mg	2.97E + 01	3.17E + 02	1.07E + 01	5.08E − 02	1.22E + 00	1.30E + 01	9.44E + 04	4.80E + 03	8.96E + 04
Na	1.95E + 01	2.60E + 03	1.33E + 02	6.35E − 01	8.49E − 01	1.13E + 02	6.55E + 04	4.16E + 04	2.39E + 04
K	6.66E + 00	6.07E + 02	9.11E + 01	4.34E − 01	1.70E − 01	1.55E + 01	1.31E + 04	5.71E + 03	7.44E + 03
Fe	5.13E − 01	1.70E − 01	3.32E − 01	1.58E − 03	9.18E − 03	3.05E − 03	7.08E + 02	1.12E + 00	7.07E + 02
Mn	3.43E − 01	1.00E − 02	2.92E − 02	1.39E − 04	6.24E − 03	1.82E − 04	4.82E + 02	6.69E − 02	4.82E + 02
Si	1.23E + 01	6.00E − 01	4.88E − 02	2.32E − 04	4.38E − 01	2.14E − 02	3.38E + 04	7.88E + 00	3.38E + 04
C	6.07E + 01	4.07E + 02	6.70E + 00	3.19E − 02	5.06E + 00	3.39E + 01	3.91E + 05	1.25E + 04	3.78E + 05
Cl	2.60E + 00	5.45E + 02	2.10E + 02	1.00E + 00	7.33E − 02	1.54E + 01	5.66E + 03	5.65E + 03	3.19E + 00
SO4	3.39E + 01	4.63E + 03	1.37E + 02	6.51E − 01	3.53E − 01	4.83E + 01	2.72E + 04	1.77E + 04	9.50E + 03
F	2.19E − 01	1.00E − 01	4.56E − 01	2.17E − 03	1.15E − 02	5.26E − 03	8.90E + 02	1.94E + 00	8.88E + 02
Br	2.74E − 02	1.94E + 00	7.07E + 01	3.37E − 01	3.43E − 04	2.43E − 02	2.65E + 01	8.93E + 00	1.76E + 01

	C(i) Groundwater composition 80% Syn_JO_Y	C(1) Jones Lake mean 1 m mg/l	C(1)/C(i) α	α(i)/α(Cl) π	C(0) mol/m**3	C(1) mol/m**3	Inflow flux mol/yr q	Outflow flux mol/yr s	Reaction flux mol/yr r
Ca	5.17E + 01	2.47E + 01	4.79E − 01	3.48E − 01	1.29E + 00	6.18E − 01	4.76E + 05	1.66E + 05	3.10E + 05
Mg	1.70E + 01	1.72E + 01	1.01E + 00	7.34E − 01	7.00E − 01	7.06E − 01	2.58E + 05	1.90E + 05	6.86E + 04
Na	2.08E + 00	1.95E + 00	9.39E − 01	6.83E − 01	9.03E − 02	8.48E − 02	3.33E + 04	2.27E + 04	1.05E + 04
K	1.95E + 00	1.55E + 00	7.91E − 01	5.76E − 01	5.00E − 02	3.96E − 02	1.84E + 04	1.06E + 04	7.82E + 03
Fe	3.06E − 01	8.95E − 01	2.92E + 00	2.13E + 00	5.48E − 03	1.60E − 02	2.02E + 03	4.31E + 03	− 2.28E + 03
Mn	7.80E − 01	3.70E − 02	4.75E − 02	3.45E − 02	1.42E − 02	6.73E − 04	5.24E + 03	1.81E + 02	5.06E + 03
Si	1.31E + 01	4.81E + 00	3.67E − 01	2.67E − 01	4.66E − 01	1.72E − 01	1.72E + 05	4.61E + 04	1.26E + 05
C	4.58E + 01	2.79E + 01	6.10E − 01	4.44E − 01	3.82E + 00	2.33E + 00	1.41E + 06	6.25E + 05	7.84E + 05
Cl	3.91E − 01	5.38E − 01	1.37E + 00	1.00E + 00	1.10E − 02	1.52E − 02	4.07E + 03	4.07E + 03	2.30E + 00
SO4	2.90E + 00	8.70E − 01	3.00E − 01	2.18E − 01	3.02E − 02	9.06E − 03	1.11E + 04	2.43E + 03	8.72E + 03
F	6.43E − 02	8.97E − 02	1.40E + 00	1.02E + 00	3.38E − 03	4.72E − 03	1.25E + 03	1.27E + 03	− 1.94E + 01

Assumed Jones Lake inflow composition is a weighted average of shallow groundwater (minipiezometer) compositions. Assumed Evans Lake inflow composition is a mix of shallow groundwater compositions and deeper groundwater (the Cone well) weighted according to $^{87}Sr/^{86}Sr$ mixing calculations.

in the groundwater flow system define a similar field, with one high-$\delta^{13}C$ outlier likely due to nonstandard sampling procedures that allowed degassing.

Evans Lake data from 1 m water depth describe a narrowly defined field in $pCO_2/\delta^{13}C_{DIC}$ space, with apparent pCO_2 two to four times atmospheric, and $\delta^{13}C_{DIC}$ compositions around +1.8 (± 0.8) ‰. Near-bottom samples range from the 1-m field up to 25 times atmospheric pCO_2, $\delta^{13}C_{DIC}$ declines with increasing pCO_2 to near −5‰. Jones Lake samples straddle atmospheric equilibrium in pCO_2, with summer conditions frequently below atmospheric partial pressure. $\delta^{13}C_{DIC}$ ranges from −6 to −2‰ but shows no clear correlation to pCO_2. Deepwater (11 m) samples exceed atmospheric pCO_2 by one to two orders of magnitude and display increasing $\delta^{13}C_{DIC}$ values (-6 to −1‰) with increasing pCO_2.

Depth profiles of apparent pCO_2, $\delta^{13}C_{DIC}$, and DIC concentration lend additional detail to the picture of lake CO_2 under different seasonal conditions. Freshwater Jones Lake showed a two order of magnitude gradient in pCO_2 with depth during strong thermal stratification in August 2000 (Fig. 11a). $\delta^{13}C_{DIC}$ showed a distinct midwater minimum, with $\delta^{13}C$ values increasing down the water column by ~2‰ to the sediment-water interface. DIC was near 1.75 mmol/L in epilimnetic water, increasing downward by a factor of ~2 through the hypolimnion. Under the more nearly mixed, late-winter conditions of March 2001, shallow pCO_2 is enhanced more than tenfold relative to August 2000. "Deep" pCO_2 is reduced, and the range in $^{13}C_{DIC}$ with water depth is expanded by 3.4‰ through both lower shallow water values and higher values near the sediment interface. DIC concentrations near 3 mmol/L in the upper 6 m increased downward to ~5.5 mmol/L near the sediment interface.

Evans Lake pCO_2 profiles (expanded in Fig. 11b) are comparatively subdued; the stratified conditions of August 2000 resulted in only a twofold range in apparent pCO_2 with maximum near-sediment values 2.5 times greater than atmospheric. Under the nearly homogenous winter water column conditions of March 2001, apparent pCO_2 showed a low-amplitude maximum in near-surface waters. $\delta^{13}C_{DIC}$ declined with depth under both summer and winter conditions, with a broader range under stratified conditions. Under summer stratification, epilimnetic DIC concentrations were near 29 mmol/L, increasing downward only 15% to near 33 mmol/L. Seasonal DIC change was also proportionately small. Winter concentrations near 31.5 mmol/L in the upper water column increased by ~5% near the sediment interface.

4.5. Carbonate Mineral Equilibria

Time series of mineral equilibria show Evans Lake in a consistent state of moderate supersaturation with $CaCO_3$ phases (Fig. 12a). Magnesite exhibits a high degree of super-

Table 3. Lead-210 activity data, age results, sedimentation rates and age errors for the Evans Lake and Jones Lake cores.

Mean depth cm	Unsupported ^{210}Pb activity pCi/gm	Cumulative dry mass (g/cm2)	Calendar yr	Sed acc rate (g/cm2/yr)	Error of age	Error of sed rate
			Evans Lake ^{210}Pb data			
1	8.0693	0.0474	1995.9	0.0291	1.71	0.00148
3			*1993.6*	*0.0252*	*1.77*	*0.0023*
5	9.5087	0.172	1990.4	0.0214	1.87	0.00103
7			*1986.7*	*0.0208*	*1.99*	*0.00189*
9	8.1128	0.3381	1982.2	0.0198	2.18	0.00121
11			*1977*	*0.0172*	*2.45*	*0.00112*
13	7.9766	0.5198	1970.7	0.0145	2.87	0.00112
15			*1964.9*	*0.0171*	*2.51*	*0.00557*
17	3.9068	0.7229	1959.9	0.0207	2.85	0.0017
19			*1955.1*	*0.0222*	*3.02*	*0.00488*
21	2.4774	0.9382	1950.6	0.0242	3.41	0.00238
23			*1944.2*	*0.0184*	*4*	*0.0027*
25	3.0713	1.182	1934.4	0.0129	5.31	0.00183
27			*1922.9*	*0.0165*	*2.28*	*0.00722*
29	0.906	1.6251	1911.3	0.0219	2.98	0.00174
31			*1898.5*	*0.0164*	*3.95*	*0.00206*
33	0.7538	2.0015	1884.5	0.0119	5.89	0.00179
35			*1871.3*	*0.0121*	*4.8*	*0.0047*
37	0.2832	2.3133	1860.6	0.0142	6.55	0.00256
39			*1847.8*	*0.0123*	*8.89*	*0.00371*
41	0.1766	2.6349	1831.6	0.0101	14.45	0.00365
			Jones Lake ^{210}Pb data			
1	24.9316	0.0976	1993.2	0.0227	1.05	0.00086
3			*1990.9*	*0.025*	*1.01*	*0.00463*
5	16.7442	0.1668	1990.5	0.0293	1.01	0.00097
7			*1988.7*	*0.0305*	*1.03*	*0.00246*
9	14.3667	0.3182	1985.5	0.0305	1.09	0.00121
11			*1982.3*	*0.0327*	*1.02*	*0.00502*
13	10.2606	0.541	1978.9	0.0349	1.08	0.00103
15			*1975.6*	*0.0341*	*1.11*	*0.00286*
17	8.7298	0.7652	1972.3	0.0333	1.17	0.00143
19			*1969.2*	*0.0366*	*1.11*	*0.00639*
21	5.9358	0.989	1966.5	0.0405	1.17	0.00133
23			*1964.1*	*0.053*	*0.91*	*0.01711*
25	2.9359	1.252	1962.1	0.0707	0.94	0.00205
27			*1960.2*	*0.0722*	*0.95*	*0.0061*
29	2.49	1.5335	1958.3	0.0739	0.97	0.0025
31			*1955.6*	*0.0725*	*1*	*0.0042*
33	2.2383	1.9817	1951.9	0.0694	1.06	0.00222
35			*1947.8*	*0.0651*	*1.11*	*0.00412*
37	1.9907	2.5399	1943	0.0602	1.22	0.00233
39			*1937.6*	*0.0544*	*1.32*	*0.00358*
41	1.7709	3.136	1931.3	0.0481	1.51	0.00225
43	1.5865	3.4394	1924.4	0.0437	1.77	0.00268
45	2.2077	3.7449	1911.2	0.0231	2.52	0.00151
47	1.0176	4.1014	1900.9	0.0346	3.36	0.00339
49	0.433	4.5089	1894.3	0.0624	4.05	0.00809
51			*1887.7*	*0.0602*	*4.75*	*0.01309*
53	0.3041	5.3054	1880.9	0.0588	5.79	0.01089
55			*1874.5*	*0.0555*	*6.92*	*0.01423*
57	0.2239	5.9753	1868.7	0.0537	8.25	0.01432
59			*1863*	*0.0527*	*9.74*	*0.01789*
61	0.1603	6.5559	1857.7	0.0529	11.45	0.01925

Open symbols are values interpolated according to the constant rate of supply (CRS) model. Supported ^{210}Pb is calculated as .32 pCi/g in both cores. 1-σ age errors were calculated by first-order error analysis of counting uncertainty (Binford, 1990).

saturation; temperature dependence of hydromagnesite equilibrium results in widely varying saturation state. No authigenic Mg-carbonate minerals have been identified in Evans Lake sediment, although dilution by the dominant $CaCO_3$ phases may mask subordinate occurrences of other authigenic minerals. Gypsum and all other sulfate minerals remain far below

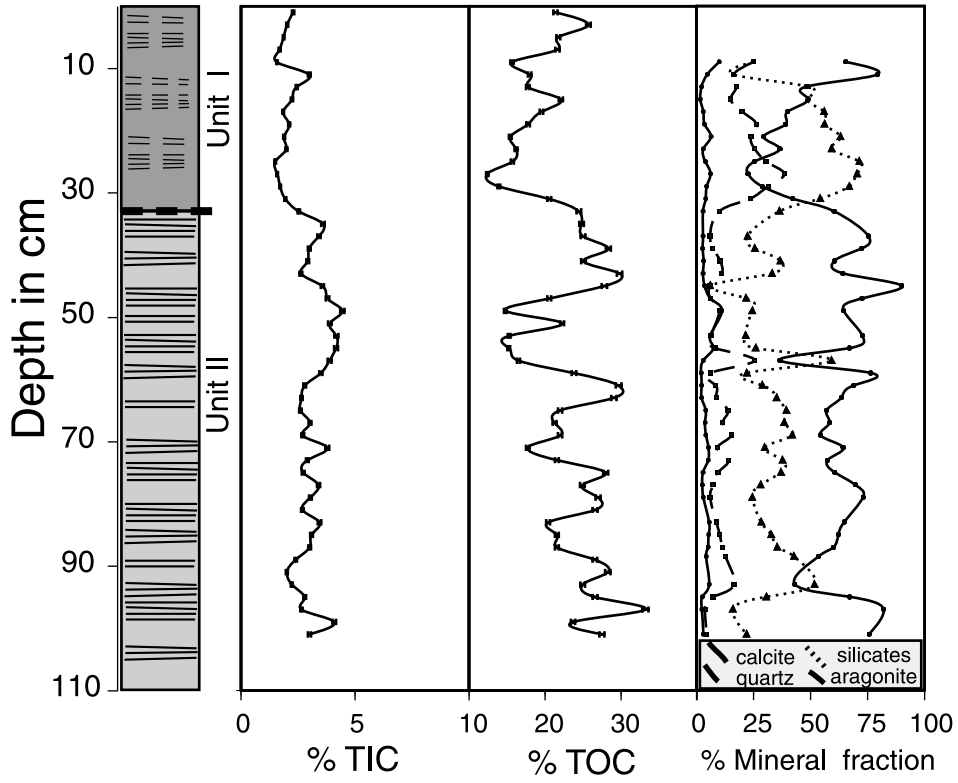

Fig. 7. Carbon stratigraphy and mineralogy of the Evans Lake short core.

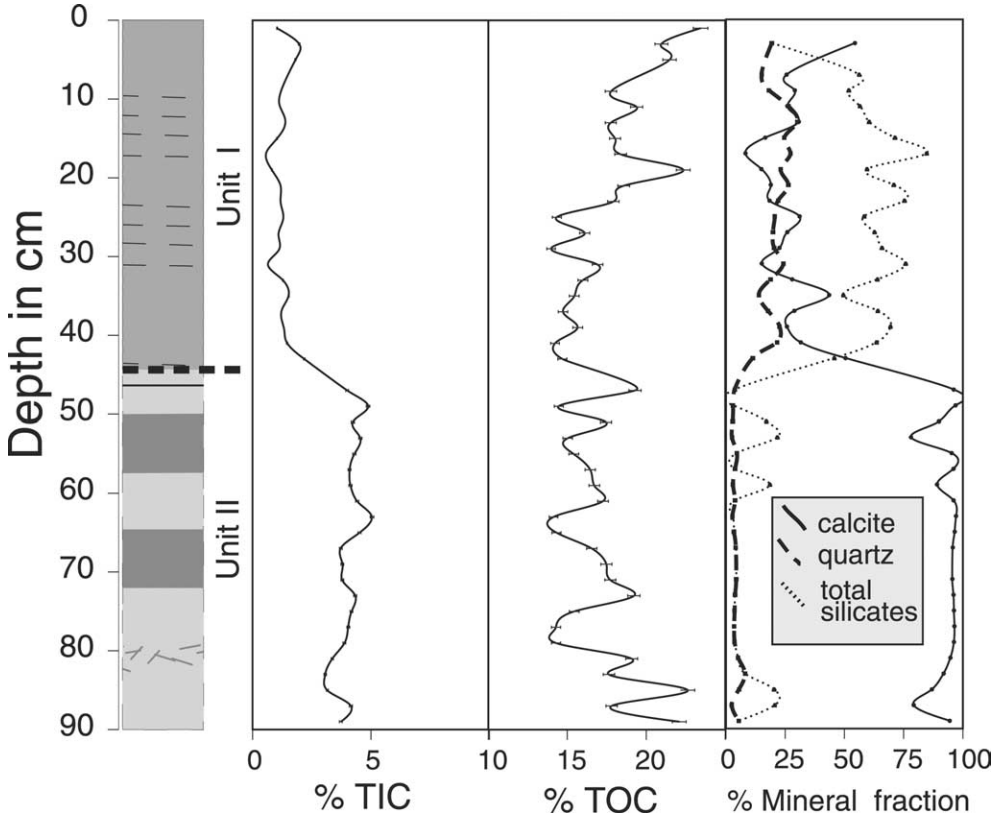

Fig. 8. Carbon stratigraphy and mineralogy of the Jones Lake short core.

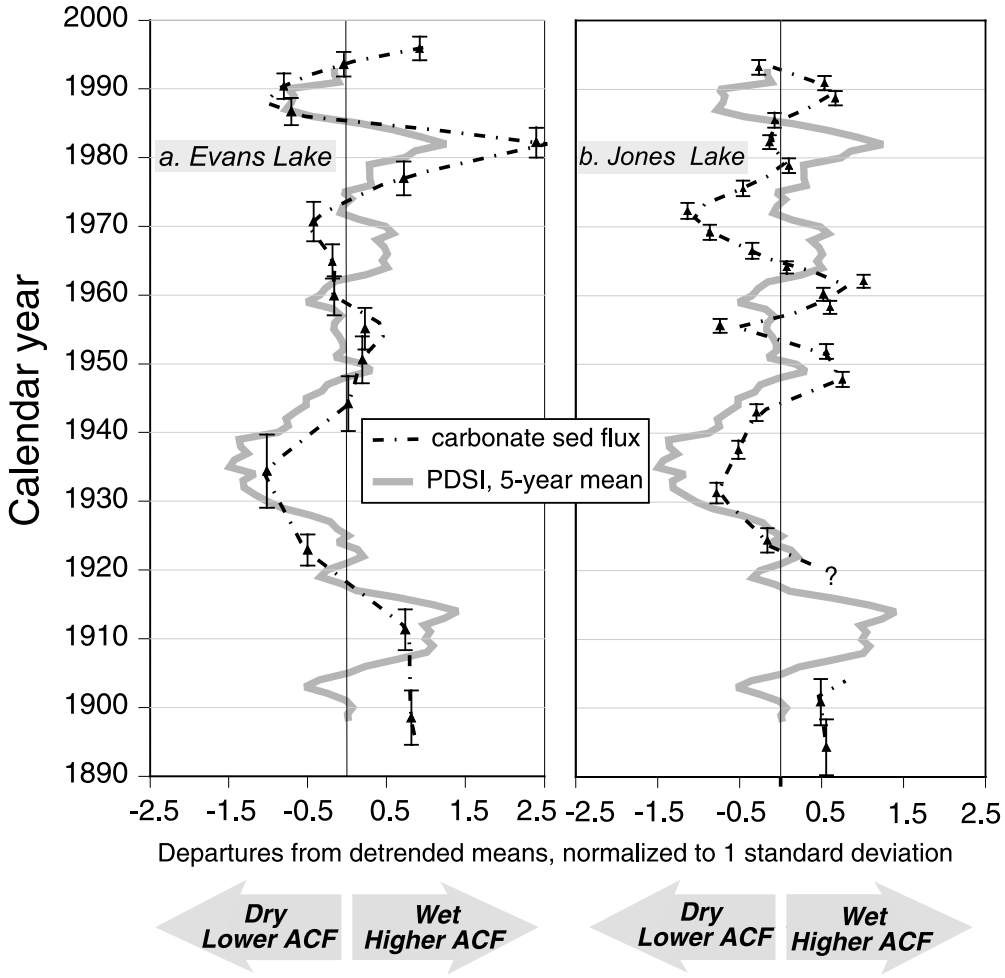

Fig. 9. Reconstructed Palmer Drought Severity Index (PDSI) and authigenic carbonate flux (ACF) for Evans Lake (a) and Jones Lake (b). PDSI and ACF are expressed as departures from detrended mean values for the period of record, normalized to standard deviations of the PDSI and ACF means.

saturation. Lowest carbonate mineral saturation index (SI) values occur in near-bottom waters during pronounced stratification of the lake water column, as a result of CO_2 accumulation and pH depression below the chemocline. With the exception of a single analysis, the water column remains above saturation with aragonite (and calcite) at both 1 m and near-bottom depths.

Jones Lake displays mineral saturation patterns more characteristic of dilute temperate lakes (Dean and Megard, 1993). $CaCO_3$ phases exceed saturation mainly during warm water conditions of inferred high-algal productivity and CO_2 drawdown (Fig. 12b). Magnesium carbonate phases remain mostly below saturation. Near-bottom waters are typically undersaturated with $CaCO_3$ phases, both during summer stratification and under winter ice cover, when the entire water column may achieve negative SI values.

5. DISCUSSION

We hypothesized a link between climate and carbonate authigenesis involving variations in areally distributed groundwater recharge. Primary geologic controls over recharge include topography, hydraulic characteristics of shallow geologic materials, and thickness of the vadose zone (Freeze and Cherry, 1979; Winter, 1983; Winter, 1999). Other important landscape controls include vegetation type and condition, timing of precipitation and snowmelt, soil and subsoil temperature, and antecedent moisture conditions (Sophocleous and Perry, 1985; Rosenberry and Winter, 1997). Mechanisms of aquifer recharge and lake-aquifer exchange within glaciated landscapes have been analyzed in theoretical, field, and numerical studies (e.g., Toth, 1962; Meyboom, 1967; Winter, 1983; Winter and Pfannkuch, 1984; LaBaugh et al., 1987; Krabbenhoft et al., 1990a; Krabbenhoft et al., 1990b; Woo and Roswell, 1993; Hayashi et al., 1998a; Hayashi et al., 1998b). Hummocky terrain generates complex groundwater flow patterns, commonly highly sensitive to recharge rate and timing. Recharge transience in such settings drives dynamic fluid, solute, and isotope fluxes between groundwater and lakes. A single hydroclimatic index cannot fully capture such a complex set of interactions. However, the PDSI water-balance model is sensitive to fundamental conditions influencing aquifer recharge (Alley, 1984; Alley, 1985), and provides a basis for a tractable test of our hypothesis.

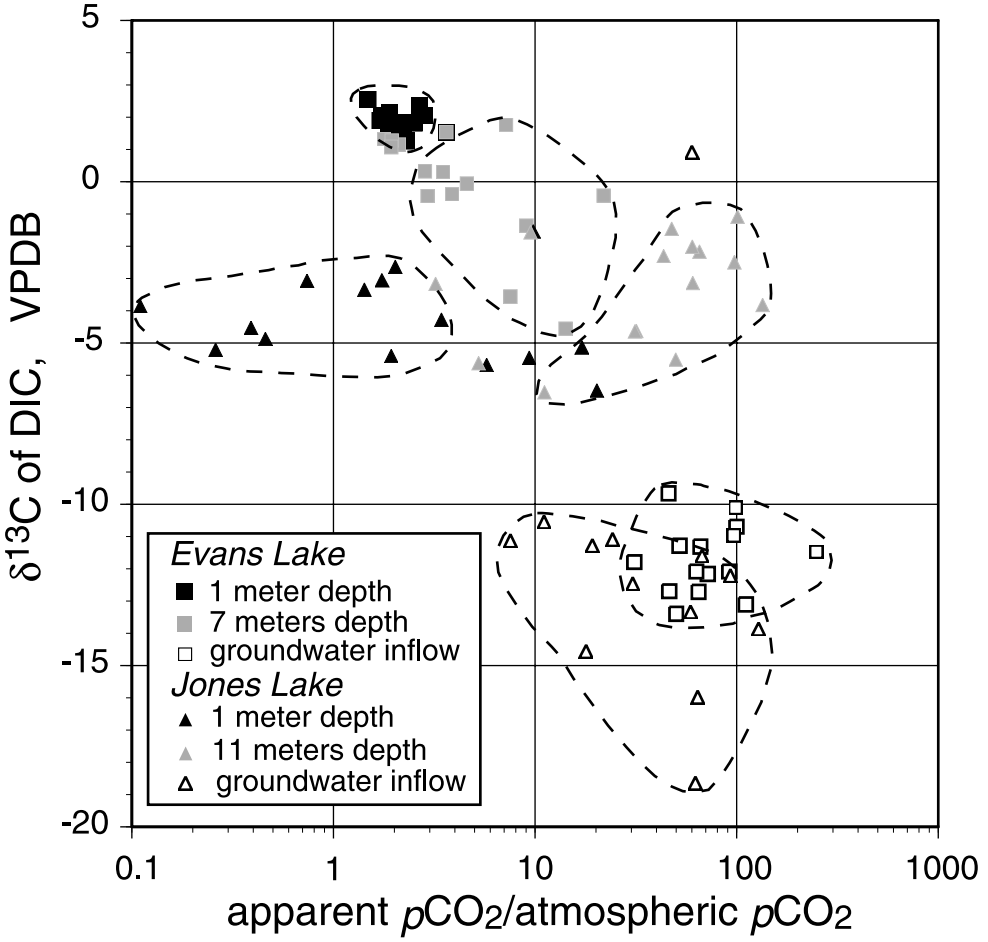

Fig. 10. Calculated pCO2 and $\delta^{13}C_{DIC}$ composition of epilimnetic and hypolimnetic lake water and of inflowing groundwater. pCO2 is normalized to atmospheric partial pressure.

Figure 9 shows the relative strength of the climate-ACF link in the two lakes. Evans Lake shows a stronger correlation than Jones Lake. Mass balance analysis of recent (1997–2001) solute partitioning helps explain the sensitivity of the climate/authigenesis link in Evans Lake (Table 2; Fig. 13). We used lake and source groundwater compositions to calculate the distribution of inflowing dissolved Ca between (1) dissolved outflow in groundwater, and (2) precipitation and sedimentation as carbonate minerals. Using a weighted mean groundwater composition based on $^{87}Sr/^{86}Sr$ mixing analysis (Figure 5; EA-2), we calculate that more than 99% of the Ca influx is reacted within the lake basin as authigenic $CaCO_3$. High alkalinity and a low rate of groundwater outflow combine to ensure that calcium export via the groundwater system is a small fraction of dissolved Ca inflow. Hence, the ACF records changes in the rate of dissolved Ca delivery from the groundwater system with considerable faithfulness.

Similar mass balance analysis explains the weaker relation between Jones Lake ACF and climate. Jones Lake water retains between 0.4 and 1.2 mmol/L Ca in solution, in contrast with Evans Lake where observed Ca concentrations are generally below 0.15 mmol/L (EA2). As a result, ~35% of calculated modern Jones Lake Ca influx is lost from the lake in groundwater outflow. As shown by pCO$_2$ and $\delta^{13}C_{DIC}$ relationships (Fig. 9), some of this Ca is initially precipitated as $CaCO_3$ under summer-elevated pH conditions but is redissolved in the hypolimnion and subsequently lost to groundwater. Sensitivity of authigenesis to changes in fluid influx is thus inherently low.

In addition, hydrologic manipulation within the Jones Lake catchment area in recent decades partially decoupled groundwater recharge rate from climate. To raise lake levels during dry yr, surface water is imported via ditch to a nearby kettle, resulting in mounding of the potentiometric surface and enhanced local groundwater fluxes. This water management strategy probably results in the contrary relationship between PDSI and mineral flux shown in the later part of the Jones Lake record.

Equilibrium geochemical modeling of simplified lake water/groundwater relationships further highlights differences in the response of carbonate flux to climate in these two lakes. We examined the distribution of groundwater-delivered Ca between aqueous and mineral phases under different mixing ratios of groundwater to lake water, using carbonate equilibria, measured aqueous geochemistry, and very simplified mineral suites. This analysis entailed the equilibration of groundwater compositions to lake pCO$_2$, followed by mixing with lake compositions in the presence of calcite in Jones Lake and aragonite in Evans Lake. Precipitation of Mg-carbonate phases

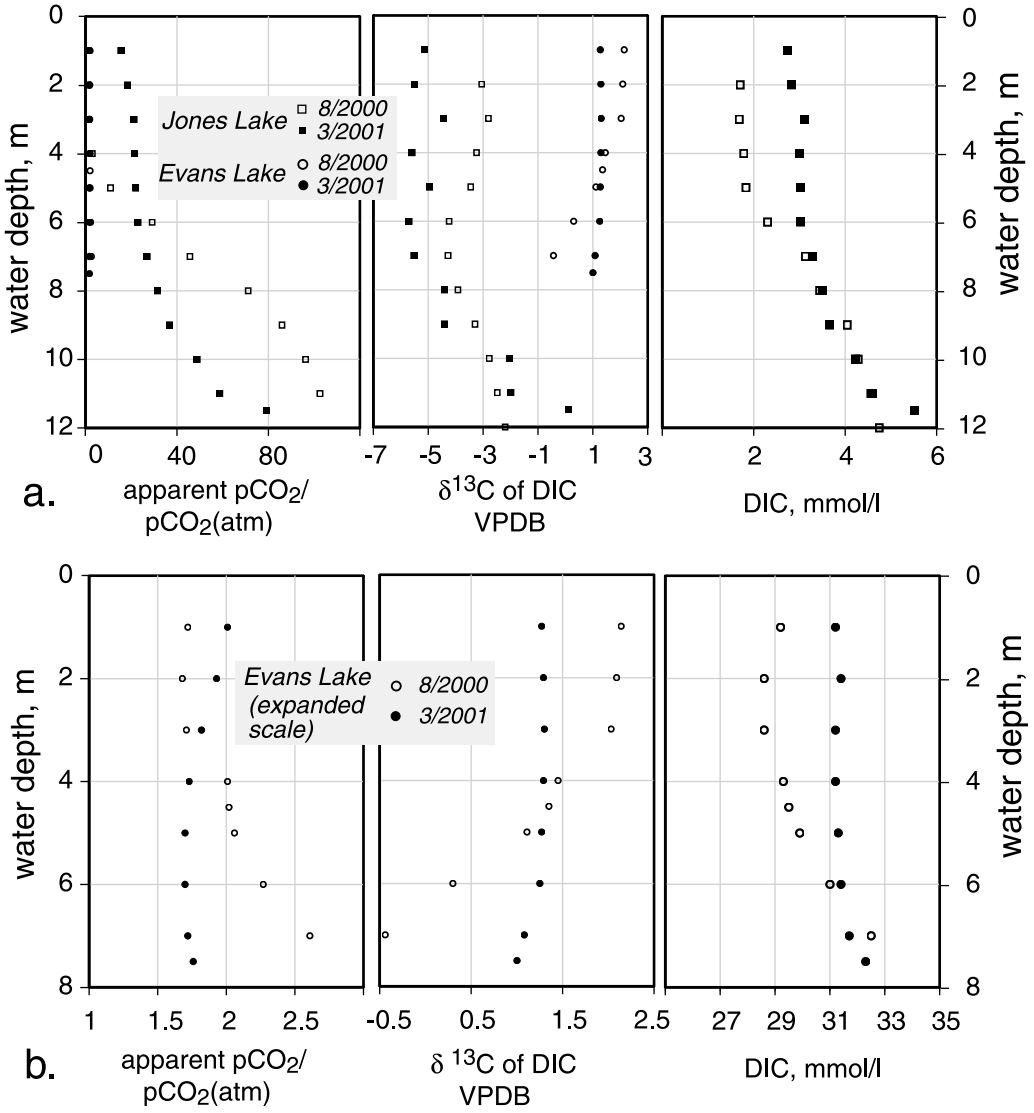

Fig. 11. Lake pCO_2, $\delta^{13}C_{DIC}$, and DIC profiles under winter and summer conditions: (a) Evans Lake and Jones Lake profiles; (b) Evans Lake data, scale expanded.

was suppressed in these experiments, as there is no lithological evidence for their occurrence in the cores. Unfavorable kinetics related to hydration strength of Mg^{2+} ions and surface charge effects typically suppress precipitation of Mg carbonates up to considerably higher ionic strength than Evans Lake presently displays (Sayles and Fyfe, 1973; Chou et al., 1989; Queralt et al., 1997; Last and De Deckker, 1990). Calcium was tracked as the fraction of groundwater-supplied Ca remaining in solution at equilibrium with different mixing ratios. Averaged groundwater compositions were calculated through simple ion-by-ion averaging of minipiezometer samples from Jones Lake and $^{87}Sr/^{86}Sr$-based weighting of minipiezometer samples and the Cone well for Evans Lake. When the modeled CO_2 equilibration paths of these average compositions are compared to measured groundwater compositions, they follow similar $CaCO_3$ precipitation pathways, supporting use of the averaged inflow compositions assumed in this analysis.

Analyses of lake-groundwater mass balance indicate contrasting allocation of solute influx between water column (eventually outflow) and sediment. Likewise, simulated mixing and equilibration of these groundwater compositions with lake water chemistry leads to differing predictions of Ca fate for the two lakes. We evaluated the mixing and equilibration of averaged groundwater inflow compositions under both "atmospherically open" (summertime lake composition, low pCO_2) and "atmospherically closed" (wintertime lake composition, high pCO_2) assumptions. In Evans Lake, both atmospherically open and atmospherically closed equilibrations of mixed compositions predict most Ca contributed by groundwater inflow should go into aragonite formation (Fig. 14a). Lake water alkalinity is high enough to produce aragonite saturation in mixed compositions at all observed lake pCO_2. This suggests that carbonate authigenesis in Evans Lake may be a year-round process. Active hypolimnetic sulfur cycling (evidenced by H_2S production and high concentrations of purple sulfur bacteria in the water column) strongly suggests that sulfate reduction contributes HCO_3^- to lake water

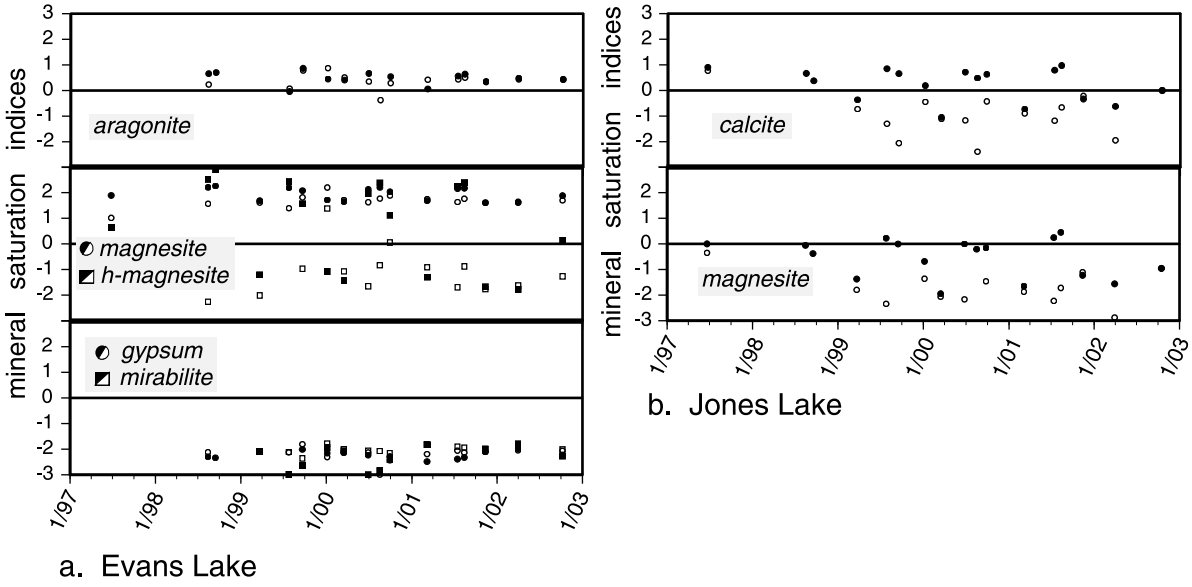

Fig. 12. Time series of selected mineral saturation indices for epilimnetic (closed symbols) and hypolimnetic (open symbols) lake waters.

through organic matter mineralization (Fenchel et al., 1998). This alkalinity production may contribute to aragonite precipitation. Even under winter ice cover when pCO_2 tends to be at its highest and pH at its lowest, more than 90% of calculated Ca inflow at annualized mixing ratios near those inferred (groundwater:lake $<<1$) would be precipitated as aragonite if exact thermodynamic equilibrium ($SI_{arag} = 0$) was maintained. Even at much higher groundwater inflow rates (groundwater/lake ~ 1), calculated Ca precipitation is $\sim$90% of inflow. For all probable mixtures, high rates of Ca removal are still expected despite the effects on ion activities of lake dilution by groundwater. Under more atmospherically open summertime conditions, an even larger fraction of inflowing Ca is expected to precipitate as $CaCO_3$, according to equilibrium calculations. These results support the interpretation, based on the PDSI-ACF comparison, of close coupling between authigenic carbonate flux and climate in this lake. An implication is that annual variation in ACF may be driven more by seasonality of groundwater inflow and the activity of the sulfate reduction cycle than by seasonality in primary production.

In Jones Lake, mixing under atmospherically open lake

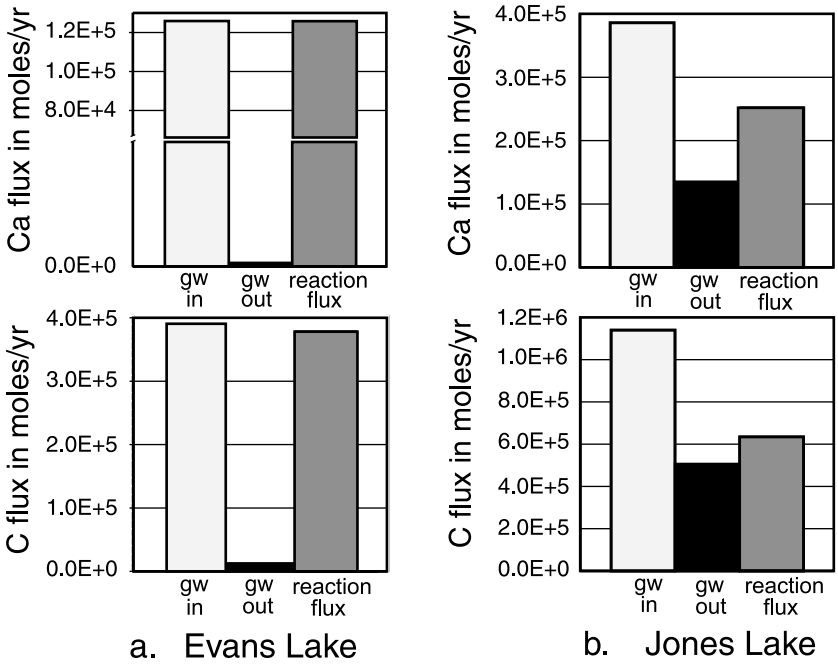

Fig. 13. Calculated steady-state disposition of groundwater derived solutes in Evans Lake (a) and Jones Lake (b).

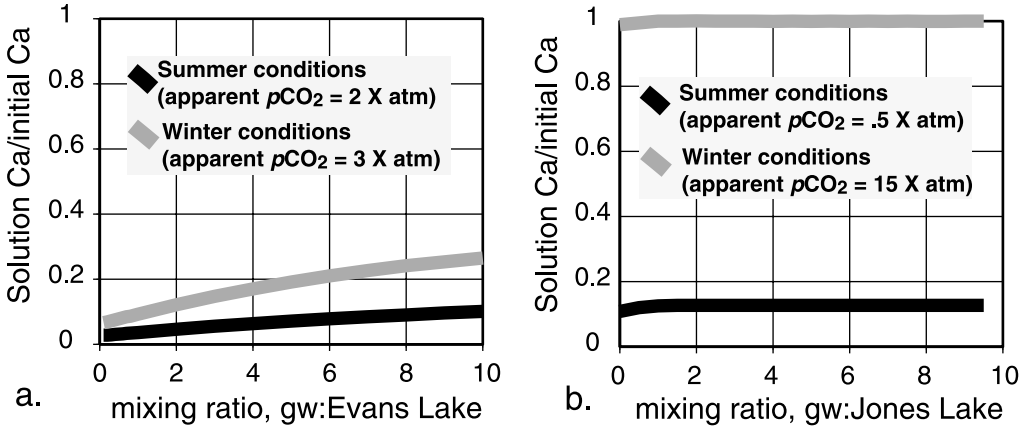

Fig. 14. Seasonal variation in calculated Ca scavenging by equilibrium $CaCO_3$ precipitation from inflowing groundwaters mixing with characteristic lake compositions: (a) Evans Lake; (b) Jones Lake.

conditions results in precipitation of ~80 to 90% of dissolved Ca as calcite, but under atmospherically closed lake conditions undersaturation of calcite results (Fig. 14b). This suggests a seasonally sensitive summertime formation process for authigenic calcite promoted by photosynthetic CO_2 depletion and is consistent with the observed weak correlation of ACF to PDSI observed for this lake.

Intralake cycling of carbon as inferred from $\delta^{13}C_{DIC}$ supports our concept of the contrasting $CaCO_3$ fluxes in the two lakes. Groundwater inflow compositions between −10 and −14‰ VPDB characterize both lakes and reflect mixing of soil-carbon derived DIC, with DIC from dissolution of carbonate minerals encountered along groundwater flowpaths. Atmospheric equilibration and photosynthetic fractionation produce more positive $\delta^{13}C$ values in both lakes. In Evans Lake, water column profiles and paired 1 m and 7 m samples show the DIC near the sediment interface to be always more negative in $\delta^{13}C$ than the rest of the water column. This $\delta^{13}C$ gradient is consistent with remineralized organic matter low in $\delta^{13}C$ providing a flux of CO_2 from near the sediment-water interface, while authigenic carbonates settling through the water column are preserved (e.g., Wachinew and Rozanski, 1997). Further support for this idea is provided by Evans Lake mineral equilibria showing hypolimnetic waters at or above aragonite saturation under almost all sampled conditions.

In Jones Lake, the DIC flux from the sediment has high $\delta^{13}C$ relative to water column values. Enhanced $\delta^{13}C_{DIC}$ at depth suggests a significant DIC flux from redissolution of authigenic calcite. As in Evans Lake, $\delta^{13}C_{DIC}$ relationships are consistent with mineral equilibria that show near-bottom waters in Jones Lake to be undersaturated under most conditions.

The calculation of ACF is potentially subject to error through inclusion of detrital calcite in the measured TIC. Several lines of evidence show this error to be small or negligible for these sediments. In Evans Lake, most of the $CaCO_3$ present is aragonite, for which there is no detrital source in this area. Moreover, the abundance of calcite in the Evans Lake core does not covary with quartz, which is present as a detrital phase. This indicates that very little detrital calcite is delivered from the landscape to Evans Lake, or by implication, to Jones Lake since the lithologies of glacial materials in the two watersheds are similar. Finally, petrographic examination of smear slides of Jones Lake unit I reveals abundant calcite of apparent authigenic origin (monocrystalline subhedral and euhedral forms) and few detrital calcite grains.

Evans Lake ACF is closely coupled to recent climate because lake DIC is high (limiting dissolved Ca activity), lake outflow is small, noncarbonate Ca-bearing mineral phases are unimportant to mass balance, and preservation of authigenic carbonate minerals is complete or nearly so. We suggest these conditions apply to Evans Lake over a rather wide climatic range. Conditions more strongly evaporative than the 20th century are unlikely to decouple ACF from climate until lake salinities much higher than the present are reached. This is because the TIC/Ca of groundwater inflow, governed by calcite dissolution and soil respiration, is likely to maintain a molar TIC excess as observed today, resulting in continued $CaCO_3$ precipitation and Ca depletion from lake waters.

Sustained conditions much less evaporative than the 20th century may weaken the Evans Lake ACF link with climate by increasing Ca export. A shift in fluid balance toward proportionally greater groundwater outflow, possible under sustained conditions of higher inflow and/or lower evaporation, will result in proportionally greater export of solutes. Evans Lake would begin to spill after a sixfold increase from its current volume. Surface water outflow would likely result in an abrupt decrease in ACF/recharge sensitivity. Lowering of lake DIC through reduced evaporative forcing or interruption of the presently active sulfate reduction cycle may also result in more Ca remaining in solution for possible export in groundwater outflow. While the sensitivity of Evans Lake ACF to such large-amplitude change is uncertain, we note that the 20th century record encompasses one highstand (1908–1915) during which lake volume exceeded the highest volume observed during our study by a factor of ~2.6, indicating climate-sensitive response in ACF persists over a rather broad range in lake conditions.

Correlation of the 20th century ACF record to climate rests on a quasi-continuous ^{210}Pb chronology and ^{210}Pb derived sedimentation rates. The ^{210}Pb chronology serves to demonstrate the mechanism linking climate variation and carbonate mineral production in groundwater-controlled lakes. Coarser chronological control, as is typical of longer records, will allow

resolution of correspondingly long-term average changes in ACF and inferred groundwater flux, while a highly resolved chronology (e.g., a varve count) will support interpretation of hydrologic change at annual or near-annual scales.

6. CONCLUSIONS

In this study, we used 20th century sediment mineralogy and carbon chemistry to calculate carbonate mass accumulation rates in two groundwater-dominated lakes. Carbonate mass accumulation rates were then used to test for a relationship between authigenic carbonate flux (ACF) and PDSI, a proxy for areally distributed groundwater recharge. ACF rates correlate with climate, with enhanced carbonate mineral production corresponding to wet climatic periods, as measured by PDSI reconstruction. Correspondence between ACF and PDSI is much more pronounced in alkaline and saline Evans Lake than in freshwater Jones Lake. Analyses of lake ionic composition and mineral equilibria demonstrate that elevated alkalinity of lake water is a key to recording and preserving the authigenic flux signal during thermal stratification and under winter ice cover. The alkaline lake in our study remains saturated with $CaCO_3$ during atmospherically closed-decomposition of organic matter. The fresh lake in our study becomes undersaturated during atmospherically closed conditions, redissolving Ca carbonate and diminishing the sensitivity of ACF to Ca inflow rates. pCO_2 and $\delta^{13}C$ composition of DIC in these lakes and their source groundwaters supports the solubility mechanism we propose to account for the contrast in ACF history between lakes. Mineral equilibria, pCO_2, and $\delta^{13}C_{DIC}$ relationships underscore the importance of year-round mineral saturation for the application of ACF as a paleorecharge estimator. Sulfate reduction contributes to the process through mineralization of organic matter to HCO_3^-. In appropriate paleolimnological settings, the mass flux rate of authigenic $CaCO_3$, limited by cation supply, is a valuable paleoclimatic proxy reflecting aquifer recharge to the groundwater catchment supplying the lake.

Acknowledgments—We wish to thank Larry Benson, Avner Ayalon, and an anonymous reviewer for careful critiques of this manuscript, which benefited in important ways from their suggestions. We also thank Eric Grimm and Dan Engstrom for critical contributions to core recovery and sediment dating. Geof and Kathy Foote, Jim and Colleen Stone, Gary and Sharon Jacobsen, and Price, Laura, and Justin Williams provided generous access to private lands and invaluable logistical assistance in the field. The senior author's contribution to this research was supported by the U.S. National Science Foundation through the University of Minnesota Department of Geology and Geophysics GeoFluids Program and the UM Paleorecords Research Training Group, and by the U.S. Department of Education through the UM Department of Geology and Geophysics GAANN Program. Critical support was provided by facilities and personnel of LRC LacCore facility. This is Limnological Research Center Contribution #601.

Associate editor: M. Bar-Matthews

REFERENCES

Alley W. M. (1984) The Palmer drought severity index: Limitations and assumptions. *J. of Climate and Applied Meteorology* **23,** 1100–1109.

Alley W. M. (1985) The Palmer drought severity index as a measure of hydrologic drought. *Water Resources Bulletin* **21** (*1*), 105–114.

Appleby P. G. (2001) Chronostratigraphic techniques in recent sediments. In *Tracking Environmental Change Using Lake Sediments, Volume 1: Basin analysis, coring, and chronological techniques* (ed. W. M. Last and J. P. Smol). pp. 171-203. Kluwer Academic Publishers.

Appleby P. G. and Oldfield F. (1978) The calculation of lead-210 dates assuming a constant rate of supply of unsupported 210Pb to the sediment. *Catena* **5,** 1–8.

Benson L. V., White L. D., and Rye R. (1996) Carbonate deposition, Pyramid Lake subbasin, Nevada: 4. Comparison of the stable isotope values of carbonate deposits (tufas) and the Lahontan lake-level record. *Paleogeography, Paleoclimatology, Paleoecology* **122,** 45–76.

Bethke C. M. (2002) *The Geochemists Workbench: A User's Guide to Rxn, Act2, React, and Gtplot.* University of Illinois.

Binford M. W. (1990) Calculation and uncertainty analysis of 210Pb dates for PIRLA project lake sediment cores. *J. of Paleolimnology* **3,** 253–267.

Bryson R. A. and Hare F. K. (1974) *Climates of North America.* Elsevier.

Chou L., Garrels R. M., and Wollast R. (1989) Comparative study of the kinetics and mechanisms of dissolution of carbonate minerals. *Chem. Geol.* **78,** 269–282.

Cook B. J. (2001) *Temporary Hydrologic Connections Make 'Isolated' Wetlands Function at the Landscape Scale.* Ph.D., University of Montana, 70p.

Cook E. R., Meko D. M., Stahle D. W., and Cleaveland M. K. (1999) Drought reconstructions for the continental United States. *J. of Climate* **12,** 1145–1163.

Dea P. A. (1981) Glacial *Geology of the Ovando Valley, Powell County, Montana.* Master's Thesis, University of Montana.

Dean W. E. (1981) Carbonate minerals and organic matter in sediments of modern North American hardwater lakes. *SEPM Special Publication* **31,** 213–231.

Dean W. E. and Megard R. O. (1993) Environment of deposition of CaCO3 in Elk Lake, Minnesota. In *Elk Lake, Minnesota: Evidence for Rapid Climate Change in the North-Central United States,* USGS Special Paper 276 (ed. J. P. Bradbury and W. E. Dean), pp. 97–113, United States Geologic Survey.

Donovan J. J. (1992) *Geochemical and Hydrologic Dynamic in Evaporative Groundwater-Dominated Lakes of Glaciated Montana and North Dakota.* Ph.D., Pennsylvania State University.

Donovan J. J. (1994) On the measurement of reactive mass fluxes in evaporative groundwater-source lakes. In *Sedimentology and Geochemistry of Modern and Ancient Saline Lakes: SEPM Special Publication No. 50* (ed. R. W. Renaut and W. M. Last), pp. 33–50, Society for Sedimentary Geology.

Donovan J. J., Smith A. J., Panek V. A., Engstrom D. R., and Ito E. (2002) Climate-driven hydrologic transients in lake sediment records: calibration of groundwater conditions using 20th Century drought. *Quaternary Science Rev.* **21,** 605–624.

Eugster H. P. and Hardie L. A. (1978) Saline Lakes. In *Physics and Chemistry of Lakes* (ed. A. Lerman), pp. 237–293, Springer-Verlag.

Eugster H. P. and Jones B. F. (1979) Behavior of major solutes during closed-basin brine evolution. *American J. of Science* **279,** 609–631.

Faure G. (1986) Principles of Isotope Geology, pp. 141–153. John Wiley and Sons.

Fenchel T., King G. M., and Blackburn T. H. (1998) *Bacterial Biogeochemistry: The Ecophysiology of Mineral Cycling.* Academic Press.

Freeze R. A. and Cherry J. A. (1979) *Groundwater.* Prentice-Hall.

Fritz P., Reardon E. J., Barker J., Brown R. M., Cherry J. A., Killey R. W. D., and McNaughton D. (1978) The carbon isotope geochemistry of a small groundwater system in northeastern Ontario. *Water Resources Research* **14,** 1059–1067.

Graber E. R. and Aharon P. (1991) An improved microextraction technique for measuring dissolved inorganic carbon (DIC), $\delta^{13}C$ and $\delta^{18}O_{H2O}$ from milliliter-sized water samples. *Chem. Geol.* **94,** 137–144.

Hardie L. A. and Eugster H. P. (1970) The evolution of closed-basin brines. *Miner. Soc. of America Special Publications* **3,** 273–290.

Hayashi M., Kamp G. v. d., and Rudolph D. L. (1998a) Water and solute transfer between a prairie wetland and adjacent uplands, 1. Water balance. *J. of Hydrology* **207,** 42–55.

Hayashi M., Kamp G. v. d., and Rudolph D. L. (1998b) Water and solute transfer between a prairie wetland and adjacent uplands, 2. Chloride cycle. *J. of Hydrology* **207,** 56–67.

Ito E. (2001) Application of stable isotope techniques to inorganic and biogenic carbonates. In *Tracking Environmental Change Using Lake Sediments, Volume 2: Physical and Chemical Techniques* (ed. W. M. Last and J. P. Smol). pp. 351-371. Kluwer Academic Publishers.

Keyantash J. and Dracup J. A. (2002) The quantification of drought: An evaluation of drought indices. *Bulletin of the American Meteorological Society* **83,** 1167–1180.

Krabbenhoft D. P., Anderson M. P., and Bowser C. J. (1990a) Estimating groundwater exchange with lakes: 2. Calibration of a three-dimensional, solute transport model to a stable isotope plume. *Water Resources Research* **26,** 2455–2462.

Krabbenhoft D. P., Anderson M. P., Bowser C. J., and Valley J. W. (1990b) Estimating groundwater exchange with lakes: 1. The stable isotope mass balance method. *Water Resources Research* **26,** 2445–2453.

LaBaugh J. W., Winter T. C., Adomaitis V. A., and Swanson G. A. (1987) Hydrology and chemistry of selected prairie wetlands in the Cottonwood Lake area, Stutsman County, North Dakota, 1979-82, pp. 26. U.S. Geological Survey.

Langmuir D. (1997) *Aqueous Environmental Geochemistry.* Simon & Schuster.

Last W. M. (1982) Holocene carbonate sedimentation in Lake Manitoba, Canada. *Sedimentology* **29,** 691–704.

Last W. M. (2001) Mineralogical analysis of lake sediments. In *Tracking Environmental Change Using Lake Sediments,* Volume 2: Physical and Geochemical Methods (ed. W. M. Last and J. P. Smol), pp. 143–188, Kluwer Academic Publishers.

Last W. M. and De Deckker P. (1990) Modern and Holocene carbonate sedimentology of two saline volcanic maar lakes, southern Australia. *Sedimentology* **37,** 967–981.

MAPS (2003) Montana Agricultural Potentials System Atlas, Vol. 2003. Montana Agricultural Extension Service, Montana State University, http://www.montana.edu/places/maps/. Accessed December 1, 2004.

McKenzie J. A. and Hollander D. J. (1993) Oxygen-isotope record in recent carbonate sediments from Lake Greifen, Switzerland (1750-1986): Application of continental isotopic indicator for evaluation of changes in climate and atmospheric circulation patterns. In *Climate Change in Continental Isotopic Records,* Vol. 78 (ed. P. K. Swartet al.), pp. 101–112, American Geophysical Union.

Meyboom P. (1967) Mass-transfer studies to determine the groundwater regime of permanent lakes in hummocky moraine of wetern Canada. *J. of Hydrology* **5,** 117–142.

Mock C. J. and Bartlein P. J. (1994) Spatial variability of late-Quaternary paleoclimates in the western United States. *Quaternary Research* **44,** 425–433.

Mucci A. and Morse J. W. (1983) The incorporation of Mg2+ and Sr2+ into calcite overgrowths: influences of growth rate and solution composition. *Geochim. Cosmochim. Acta* **47,** 217–233.

Queralt I., Julia R., Plana F., and Bischoff J. L. (1997) A hydrous Ca-bearing magnesium from playa lake sediments, Salines Lake, Spain. *American Mineralogist* **82,** 812–819.

Rogers D. B. and Dreiss S. (1995) Saline groundwater in Mono Lake, California: 1. Distribution. *Water Resources Research* **31,** 3131–3150.

Rosenberry D. O. and Winter T. C. (1997) Dynamics of water-table fluctuations in an upland between two prairie-pothole wetlands in North Dakota. *J. of Hydrology* **191,** 266–289.

Sanford W. E. and Wood W. (1991) Brine evolution and mineral deposition in hydrologically open evaporite basins. *American J. of Science* **291,** 687–710.

Sayles F. L. and Fyfe W. S. (1973) The crystallization of magnesite from aqueous solution. *Geochim. Cosmochim. Acta* **37,** 87–99.

Schnurrenberger D., Russell J., and Kelts K. (2003) Classification of lacustrine sediments based on sedimentary components. *J. of Paleolimnology* **29,** 141–154.

Smith A. J., Donovan J. J., Ito E., and Engstrom D. R. (1997) Groundwater processes controlling a prairie lake's response to middle Holocene drought. *Geology* **25,** 391–394.

Sophocleous M. and Perry C. A. (1985) Experimental studies in natural groundwater-recharge dynamics: the analysis of observed recharge events. *J. of Hydrology* **81,** 297–332.

Teller J. T. and Last W. M. (1990) Paleohydrologic indicators in playas and salt lakes, with examples from Canada, Australia and Africa. *Paleogeography, Paleoclimatology, Paleoecology* **76,** 215–240.

Toth J. (1962) A theory of groundwater motion in small drainage basins in central Alberta, Canada. *J. of Geophysical Research* **67,** 4375–4387.

Tuck L. K., Briar D. W., and Clark D. W. (1996) Geologic history and hydrogeologic units of intermontane basins of the Northern Rocky Mountains, Montana and Idaho. U.S. Geological Survey Hydrologic Investigations Atlas.

Wachinew P. and Rozanski K. (1997) Carbon budget of a mid-latitude, groundwater-controlled lake: Isotopic evidence for the importance of dissolved inorganic carbon recycling. *Geochim. Cosmochim. Acta* **61,** 2453–2465.

Winter T. C. (1983) The interaction of lakes with variably saturated porous media. *Water Resources Research* **19,** 1203–1218.

Winter T. C. (1999) Relation of streams, lakes and wetlands to groundwater flow systems. *Hydrogeology Journal* **7,** 28–45.

Winter T. C. and Pfannkuch H. O. (1984) Effect of anisotropy and groundwater system geometry on seepage through lakebeds. *J. of Hydrology* **75,** 239–253.

Winter T. C., LaBaugh J. W., and Rosenberry D. O. (1988) The design and use of a hydraulic potentiomanometer for direct measurements of differences in hydraulic head between groundwater and surface water. *Limnology and Oceanography* **33,** 1209–1213.

Woo M.-K. and Roswell R. D. (1993) Hydrology of a prairie slough. *J. of Hydrology* **146,** 175–207.

ELECTRONIC ANNEX

Supplementary data associated with this article can be found, in the online version, at doi:10.1016/j.gca.2004.12.001.